Local helioseismology using ring diagram analysis

H. M. Antia[1] and **Sarbani Basu**[2]

[1] Tata Institute of Fundamental Research, Homi Bhabha Road, Mumbai 400005, India
[2] Astronomy Department, Yale University, P. O. Box 208101, New haven CT 06520-8101, U. S. A.

The dates of receipt and acceptance should be inserted later

Key words Sun; helioseismology; Sun: oscillations; Sun; interior

Ring diagram analysis is an extension of global helioseismology that is applied to small areas on the Sun. It can be used to infer the horizontal components of large scale flows as well as the structure, and variations thereof, in the outer convection zone. We describe below the ring-diagram analysis technique, and some results obtained using this technique.

© 2006 WILEY-VCH Verlag GmbH & Co. KGaA, Weinheim

1 Introduction

Helioseismology has successfully determined the solar internal structure (e.g., Gough et al. 1996) as well as the rotation rate in the solar interior (e.g., Thompson et al. 1996; Schou et al. 1998). However, the low and intermediate degree modes that are used in these global studies do not resolve features near the solar surface adequately. Furthermore, the global modes are only sensitive to the east-west component of horizontal velocity (i.e. rotation). And these modes are only sensitive to the longitudinally-averaged north-south symmetric component of the rotation rate and of structure. The meridional (north-south) component of velocity cannot be studied using the global modes. Local helioseismic techniques need to be employed to study the meridional component of velocity as well as to study the longitudinal variation of solar flows and solar structure. These techniques, which are effectively based on high-degree modes of solar oscillations, also give better resolution near the solar surface when compared to global techniques. High-degree solar oscillation modes ($\ell \geq 150$) which are trapped in the outer parts of the solar envelope have lifetimes that are much smaller than the sound travel time around the Sun and hence the characteristics of these modes are mainly determined by average conditions in the local neighbourhood rather than the average conditions over the entire spherical shell. The properties of these modes are better determined by local helioseismic techniques. Ring diagram (plane wave k-ν) analysis (Hill 1988) and time-distance analysis (Duvall et al. 1993) are examples of such local helioseismic techniques. In this review we will describe only the ring-diagram analysis. For other techniques readers can refer to Gizon & Birch (2005) and other articles in this issue.

Ring diagram analysis is an extension of global helioseismic analysis with the observations being restricted to a small region (typically $15^\circ \times 15^\circ$) of the solar surface. Ring diagrams are obtained from a time series of Dopplergrams of a specific area of the Sun generally tracked with the mean rotation velocity. The Dopplergrams are remapped to heliographic co-ordinates while tracking. The three dimensional Fourier transform of this time series gives the power spectrum $P(k_x, k_y, \nu)$, where k_x, k_y are the wavenumbers in the two spatial directions and ν is the cyclic frequency. These power spectra are referred to as ring diagrams because of the characteristic ring-like shape of regions where the power is concentrated in sections of constant temporal frequency, reflecting the near azimuthal symmetry of the power in $\mathbf{k}$ space (Fig. 1). These 3D power spectra are the basic inputs for ring diagram analysis. The frequency $\nu(k_x, k_y)$ where the power is concentrated provides the diagnostic for the region studied. In particular, these frequencies are shifted due to flows in the horizontal (x, i.e., zonal, and y, i.e., meridional) directions. By measuring the frequency shifts one can, in principle, estimate the flow velocities below the surface. The frequency shifts and other parameters are a horizontal average of these parameters over the region studied. Thus the size of the chosen region determines the spatial resolution of ring diagram studies. This size in turn, is determined by the necessity of being able to resolve modes with different wavenumbers in some suitable range. For the spatial resolution of MDI (Michelson Doppler Imager) and GONG (Global Oscillations Network Group) instruments a size of $15^\circ \times 15^\circ$ is found to be reasonable for most applications.

In the next section we describe the technique used in fitting the ring diagram power spectra and the inversion techniques to infer the flows and structure variations. In Section 3, we describe some of the results that have been obtained using this technique.

2 The technique

Analysis of ring diagrams begins by fitting a model to the 3D power spectrum to determine the frequencies and other parameters. Different techniques and models have been used for this purpose (Schou & Bogart 1998; Patrón et al. 1997;

© 2006 WILEY-VCH Verlag GmbH & Co. KGaA, Weinheim

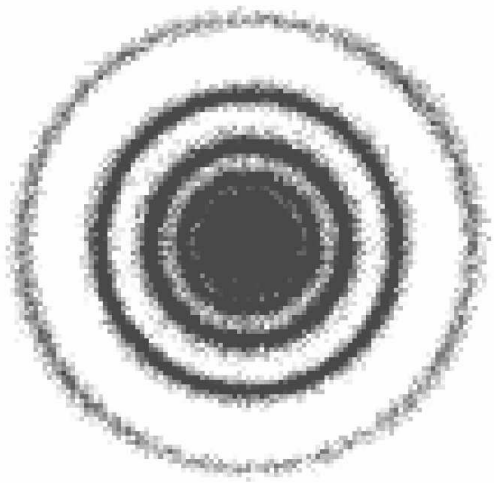

Fig. 1 The section at $\nu = 4$ mHz of a 3D power spectrum obtained from MDI data from the equatorial region. The spectrum was obtained by averaging over 8 spectra during May 1997.

Basu et al. 1999). These techniques basically use a maximum likelihood method (Anderson et al. 1990) to fit a model profile to the different rings in power spectra that correspond to different values of n. For example, Basu & Antia (1999) use the model

$$P(k_x,k_y,\nu) = \frac{e^{B_1}}{k^3} + \frac{e^{B_2}}{k^4} + \frac{\exp(A_0 + (k-k_0)A_1 + A_2(\frac{k_x}{k})^2 + A_3\frac{k_xk_y}{k^2})S_x}{x^2+1}, \quad (1)$$

where

$$x = \frac{\nu - ck^p - U_xk_x - U_yk_y}{w_0 + w_1(k-k_0)}, \quad (2)$$

$$S_x = S^2 + (1+Sx)^2, \quad (3)$$

$$k^2 = k_x^2 + k_y^2, \quad (4)$$

and the 13 parameters $A_0, A_1, A_2, A_3, c, p, U_x, U_y, w_0, w_1, S, B_1$ and B_2 are determined by fitting the spectra. This model is used to fit each ring separately in a small range of frequencies and wavenumber centred at $k = k_0$. The first two terms in Eq. (1) parametrise the background power, while the last term represents the power in modes. The parameter S measures the asymmetry in the peak profile in the form used by Nigam & Kosovichev (1998). Negative values of S imply more power on the lower frequency side of the peak. The wavenumber k is usually expressed in terms of degree of modes ($k^2 = \ell(\ell+1)/R_\odot^2$), though the degree ℓ is not restricted to be an integer. However, ultimately the analysis requires eigenfunctions from a full solar model which restricts ℓ to be an integer. Because of the finite region that is used in the study there is some lower limit on k that can be used, since below that the rings are too small to be fitted properly. This determines the depth to which the interior properties can be inferred. Increasing the size of the region will allow smaller values of k to be fitted, at the cost of horizontal resolution in the study. For large regions the plane wave assumption used in calculating power spectra may also break down.

Most ring diagram studies use a symmetric Lorentzian profile to fit the spectra. Basu & Antia (1999) found that introducing asymmetry does not change the basic results significantly. The parameters of interest here are the mean frequency $\nu = ck^p$, line-width w_0, amplitude $\exp(A_0)$, asymmetry parameter S and the velocities U_x and U_y which cause frequency shifts. The frequency can be used to study the solar structure below the surface. The line-width is determined by the life-time of the modes and can be used to study the damping mechanisms. However, some care is needed in this interpretation as a large contribution to the line-width is due to the finite resolution in wavenumber k and frequency ν (Howe et al. 2004) which needs to be accounted for when interpreting the line widths. The amplitude of the modes is determined by the competition between the excitation and damping mechanisms and therefore, can be used to study these processes. The asymmetry of the line profiles is determined by the location of the excitation sources. The sign of the asymmetry depends on whether the spectra are obtained from Doppler observations or intensity measurements. The asymmetry is generally negative for spectra obtained from velocity, and generally positive for spectra from intensity measurements. The velocities U_x and U_y can be inverted to get the zonal (east-west) and the meridional (north-south) velocity components respectively as a function of depth in the given region. From the fits we get these parameters as a function of the radial harmonic number n and the degree ℓ.

2.1 Inversions for flow velocities and structure

The ring spectra are fitted to get the parameters U_x and U_y for different modes. These represent a weighted average over depth of the corresponding velocity components u_x or u_y given by

$$U_x^{n,\ell} = \int u_x(z)\mathcal{K}_v^{n\ell}(z)\,dz, \quad (5)$$

where the kernels $\mathcal{K}_v^{n\ell}$ can be calculated using a solar model. A similar equation can be written for $U_y^{n,\ell}$ The kernels are calculated using spherical models, while the power spectra are for plane-waves, and therefore, this approximation introduces an error. The effect of this approximation has not been explored in detail, but is assumed to be small. By comparing the zonal velocity calculated from ring diagram with the mean rotational velocity at the same latitude as obtained from frequency splittings of global modes one can estimate the systematic error introduced in the study (Basu et al. 1999). It should be noted that the zonal flow velocity $u_x(z)$ represents the difference between the actual velocity and the mean rotation velocity assumed while tracking the region.

Equation (5) defines a linear inverse problem to determine the velocity $u_x(z)$ (or $u_y(z)$) when the kernels and $U_x^{n,\ell}$ (or $U_y^{n,\ell}$) are known for a set of modes. This is basically an ill-conditioned problem and we need some addi-

© 2006 WILEY-VCH Verlag GmbH & Co. KGaA, Weinheim

tional assumptions to get a reasonable solution. This is generally done by assuming that the solution is smooth in some sense. There are many techniques for solving inverse problems (Gough & Thompson 1991). The two main approaches are the Regularised Least Squares (RLS) and the Optimally Localised Averages (OLA) methods.

The basic idea of the RLS method is to expand the required solution in terms of suitable basis functions and to determine the coefficients of expansion by minimising the sum of the squared differences between the observations and the adopted model. An additional term is added to ensure smoothness of the solution. This is usually the integral of the squared second derivative. For example, we minimise a function of the form

$$\chi^2 = \sum_{n,\ell} \frac{1}{\sigma^2_{n,\ell}} \left(U_x^{n,\ell} - \int K_v^{n,\ell}(z) u_x(z)\, dz \right)^2 + \lambda \int \left(\frac{d^2 u_x(z)}{dz^2} \right)^2 dz\,. \quad (6)$$

Here we have assumed the errors, $\sigma_{n,\ell}$ to be independent of each other. The constant λ is a regularisation parameter, which is adjusted to get appropriate smoothness of the solution. If $\lambda = 0$, the solution reduces to a normal least squares approximation, while for very large values of λ the solution will approach a linear function. In particular, at large depths where only a few modes penetrate, the resulting solution will tend to be linear. For the second term of Eq. (6) we can choose to minimise the first derivative instead of the second derivative. In that case the solution will approach a constant value as $\lambda \to \infty$. The choice of λ is arbitrary to some extent, but it can be selected by experimenting with artificial data calculated for known velocity profiles with random errors (consistent with those in the observed data) added to the artificial data. The inversion results for these artificial data can then be compared with the known input profiles to estimate an optimal value of λ. If λ is properly chosen then the results are not very sensitive to small variations in this parameter.

The OLA technique (Backus & Gilbert 1968) attempts to produce a linear combination of data such that the resulting averaging kernel is suitably localised while simultaneously controlling the error estimates. The basic idea in OLA method is to construct a linear combination of data

$$u_x(z_0) = \sum_{n,\ell} a_{n,\ell}(z_0) U_x^{n,\ell} = \int \mathcal{K}(z, z_0) u_x(z)\, dz, \quad (7)$$

where $\mathcal{K}(z, z_0)$ is the averaging kernel given by

$$\mathcal{K}(z, z_0) = \sum_{n,\ell} a_{n,\ell}(z_0) \mathcal{K}_v^{n,\ell}(z)\,. \quad (8)$$

The coefficients $a_{n,\ell}(z_0)$ are selected such that the resulting averaging kernel is localised around $z = z_0$ and at the same time the error

$$\sigma^2_{u_x}(z_0) = \sum_{n,\ell} a^2_{n,\ell}(z_0) \sigma^2_{n,\ell} \quad (9)$$

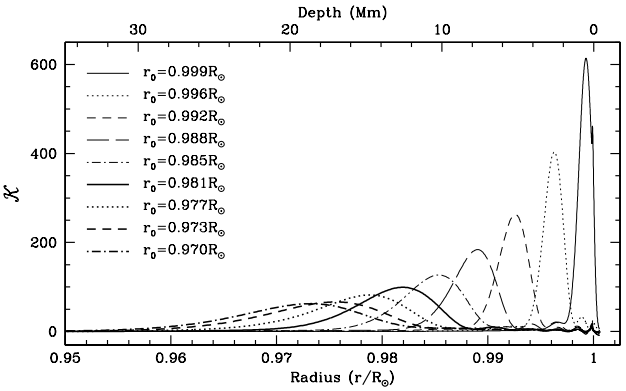

Fig. 2 A few averaging kernels for inversion of flow velocities from ring diagram analysis using the OLA technique.

on the estimated $u_x(z_0)$ is controlled. The width of the averaging kernel gives an estimate of the spatial resolution of the inversion. Once again an appropriate compromise has to be made between the conflicting requirements of low errors and high resolution (i.e., small width) of the averaging kernels. A sample of averaging kernels obtained for inversions to calculate solar flows is shown in Fig. 2. The data used are for a ring diagram analysis of the equatorial region of the Sun during Carrington Rotation 1910. The power-spectrum used was the averaged power spectrum of twenty four $15^\circ \times 15^\circ$ regions spanning the entire rotation.

The OLA technique requires significant amounts of computation and quite often a variant called Subtractive Optimally Localised Averages (SOLA) (Pijpers & Thompson 1992, 1994) is used. These techniques have been successfully used for ring diagram analysis (Basu et al. 1999; Haber et al. 2002). Comparison of results obtained using different inversion techniques gives an estimate of systematic errors involved in the inversion process (Basu et al. 1999; Haber et al. 2004).

The frequencies obtained from fitting ring diagrams can, in principle, be used to invert for structure variables like, sound speed, density and adiabatic index below the solar surface. Unlike the inversion for flow velocities, the inversion for structure variations is nonlinear and all techniques are based on linearising the equation that relates structure to frequencies using the variational principle. For structure inversions using global modes, the equations are linearised around a known solar model, and the frequency differences between the Sun and the model are inverted to obtain the difference in sound speed and density between the Sun and the model (e.g., Dziembowski et al. 1990; Antia & Basu 1994). This however, may not be acceptable for ring diagram studies, since there may be unknown systematic errors caused by approximating the spherical surface of the Sun by a plane-parallel model as well as those caused by the projection of a spherical surface onto a plane, particularly at high latitudes. As a result, in most ring diagram studies of solar structure, we take the differences between two sets of observed frequencies to study the differences in structure

© 2006 WILEY-VCH Verlag GmbH & Co. KGaA, Weinheim

between the corresponding regions. If these structural differences are small, the linearisation may be justified. Thus the difference in frequencies of two regions would be related by

$$\frac{\delta\nu_{n,\ell}}{\nu_{n,\ell}} = \int \mathcal{K}^{n,\ell}_{c,\rho}(z)\frac{\delta c^2}{c^2}(z)\,dz + \int \mathcal{K}^{n,\ell}_{\rho,c}(z)\frac{\delta\rho}{\rho}(z)\,dz + \frac{F(\nu_{n,\ell})}{I_{n,\ell}} \quad (10)$$

Here again the kernels can be calculated from a known solar model. The kernel $\mathcal{K}_{c,\rho}(z)$ measures the sensitivity of frequencies to variations in sound speed at constant density, while $\mathcal{K}_{\rho,c}(z)$ measures the effect of density at constant sound speed. The function $F(\nu)$ is a smooth function which takes into account uncertainties in layers very close to the surface, while $I_{n,\ell}$ is the mode inertia. This term is essentially *ad hoc* and takes account of various contributions from near-surface layers, such as non-adiabatic effects, that are not included in the variational principle. In addition to ignored effects, the surface term also accounts for contributions from near-surface regions that cannot be resolved by the mode set used for the inversions. Once again we can use any of the inversion techniques like RLS, OLA or SOLA for calculating the structure difference between two regions in the Sun (e.g., Basu et al. 2004).

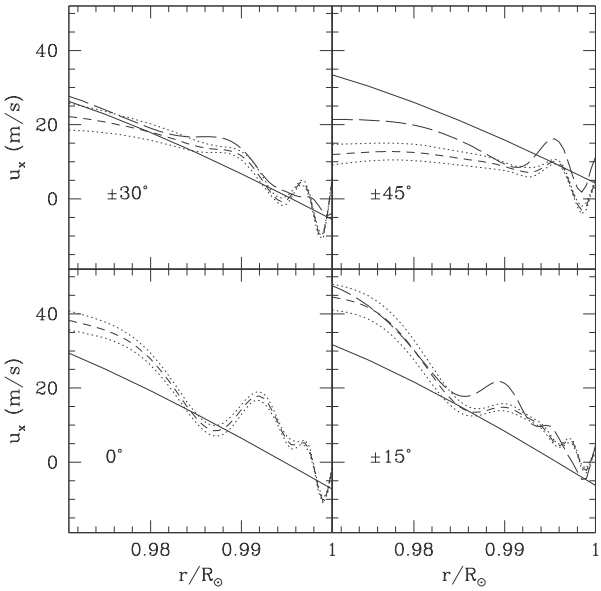

Fig. 3 The zonal velocity as calculated from ring diagram analysis from data for June 2000 is compared with the rotation velocity obtained from inversions of rotation splittings of global modes obtained for the same period. The solid lines show the rotation velocity, while the short-dashed and long-dashed lines show the zonal velocity for the north and south hemispheres respectively. The dotted lines show the errors on the north hemisphere result. The errors on other curves are not shown for clarity.

3 Results

Ring diagram analysis was proposed by Hill (1988) for studying flows in the solar interior. Hill (1989) used data obtained at NSO to study the flow velocities in four different regions on the Sun and found variations of order of 20 m s^{-1}. Subsequently, Hill (1990) applied inversion techniques to infer the flow velocities as a function of the depth from frequency shifts caused by flows. The shifts were determined by fitting ellipses to the rings at constant frequency. Patron et al. (1997) attempted to fit 3D power spectra using a Lorentzian profile, and applied this to data obtained from the Taiwan Oscillation Network (TON). With the availability of data from the MDI instrument on board SOHO, considerable progress has been made in applying ring diagram technique to study large scale flows in the solar interior. The updated GONG instruments are now providing near-continuous coverage of the Sun, and the data are being successfully used for ring-diagram analysis.

Although ring diagram analysis cannot measure the flow velocities in the vertical direction, Komm et al. (2004) have attempted to use the continuity equation to estimate the vertical component using the horizontal velocities on a grid of regions covering the solar surface. Considering the low resolution of ring diagram technique and significant uncertainties in the horizontal velocities, it is not clear if such efforts can yield reliable estimate for the vertical component of velocities, however, it is a promising start. The study of structure variations through ring-diagram analysis is also a recent development, and it is still in its infancy. We present below some of the results obtained through ring-diagram analysis.

3.1 Large scale flows

Rotation of the solar interior has been studied using global modes (e.g., Thompson et al. 1996; Schou et al. 1998). These studies have determined the rotation rate as a function of both depth and latitude. With accumulation of GONG and MDI data over the last 11 years, solar cycle-related variations of the rotation rate have also been studied extensively (e.g., Howe et al. 2000; Basu & Antia 2000a). These results can be compared with zonal flows obtained using ring diagram technique. Schou & Bogart (1998) used MDI data from 1996 May 24 through July 24 to obtain 3D power spectra and fitted the spectra to study the horizontal velocities. They found that the measured zonal flow velocity agrees with rotation velocity from global modes near the solar surface. Basu et al. (1999) applied both the RLS and OLA inversion techniques to ring diagram data to infer flow velocities as a function of depth. The zonal flow velocity profile at different latitudes obtained from ring diagram analyses was found to agree with that obtained from global mode analyses. The shear layer near the solar surface was studied in detail. They also compared the zonal flow velocities in the north and south hemispheres, and found a difference of about 5 m s^{-1} near the surface, but in view of possible systematic errors it is not clear if this can be considered to be significant. Similar results were obtained by González Hernández & Patrón (2000). Figure 3 shows a comparison of zonal velocities in the two hemispheres obtained by ring diagram analysis with rotation velocity inferred from rota-

© 2006 WILEY-VCH Verlag GmbH & Co. KGaA, Weinheim

tional splittings of global modes. While Basu et al. (1999) studied ring spectra at different latitudes that were averaged over an entire Carrington rotation to improve precision, Haber et al. (2000) used ring diagram analysis to study mosaics of regions covering entire solar surface up to a latitude of 60° (usually referred to as the 'dense-pack') at different times. They used this to study the variation in flow velocities over latitude and longitude.

Haber et al. (2000) and Basu & Antia (2000b) have identified the torsional oscillation pattern in the east-west flows. A similar pattern of temporal variation has been seen at the solar surface (Howard & LaBonte 1980) and in the interior using global modes (Howe et al. 2000; Basu & Antia 2000a). Haber et al. (2000) also found north-south asymmetry in the zonal flow velocities. Some north-south asymmetry has been found in all results, but there is no agreement between different results and it is not clear if there is indeed any significant asymmetry.

Unlike zonal flows, meridional flows cannot be determined from frequency splittings of global modes, and hence these have been inferred using local helioseismic techniques only. Surface Doppler measurements have shown meridional flows with an amplitude of about 27 m s^{-1} from the equator to the poles in both hemispheres (e.g., Hathaway et al. 1996). These flows play a crucial role in modern solar dynamo theories (e.g., Dikpati & Charbonneau 1999; Nandy & Choudhuri 2002), and hence it is important to study these flows in the solar interior. In particular, conservation of mass requires that the direction of meridional flow should reverse below some depth in the interior. Many dynamo models assume that this occurs around the tachocline, but current helioseismic technique cannot give any information about these flows at such depths.

Giles et al. (1997) were the first to detect meridional flows in the solar interior using time-distance technique. Their results agree with those obtained using ring diagram analysis (Schou & Bogart 1998; Basu et al. 1999; González Hernández et al. 1999; Haber et al. 2000). These studies did not find any evidence of a return flow from the poles to the equator up to a depth of about 21 Mm — ring-diagram analyses cannot probe deeper layers. The dominant component of the meridional flow has a form $v_m \sin(2\theta)$, where θ is the colatitude and the amplitude is found to be about 30 m s^{-1} near the surface. There is only a weak depth dependence in the amplitude of this component. Higher components are also significant at intermediate depths. In particular, the component $P_4^1(\cos\theta)$ (where $P_\ell^m(x)$ is the associated Legendre polynomial) suggested by Durney (1993) is found to have an amplitude of about 3-4 m s^{-1} (Basu et al. 1999; Basu & Antia 2003). The north-south symmetric component is generally small and the observed value could be due to instrumental effects.

Haber et al. (2002) found a submerged equatorward flow in the north hemisphere during the years 1998–2001. The cell is particularly strong during years 1999 and 2001, when these cells start at a depth of about 5 Mm. Basu & Antia

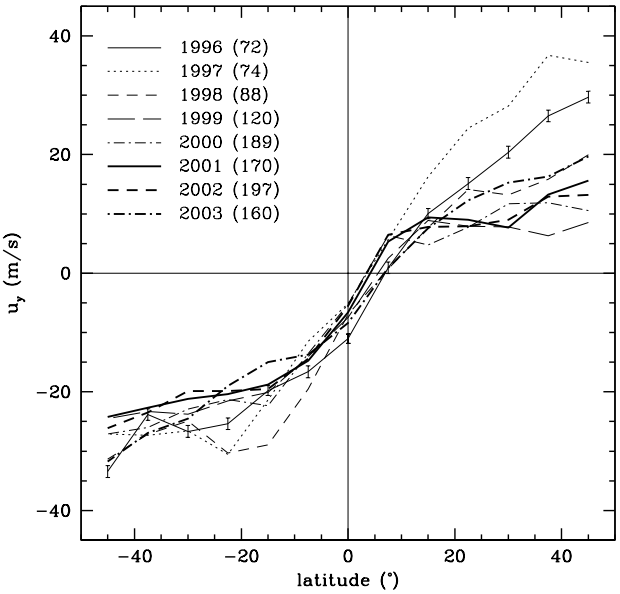

Fig. 4 The meridional flow velocity averaged over a depth range of 4–8 Mm obtained from MDI data for different years as marked in the figure. The 10.7 cm radio flux (which is a measure of solar activity) during the corresponding time is shown in units of the Solar Flux Units in parentheses.

(2003) did not find any evidence for these counter-cells during the same period using essentially the same data from MDI, and there is some evidence that this could be a problem with the way the ring spectra were obtained (see e.g., Bogart & Basu 2004). Figure 4 shows the meridional flow velocity as a function of latitude averaged over a depth range of 4–8 Mm at different times. These results do not show any counter-cell. In deeper layers there is a hint of counter-cell in 1999 data at high latitudes ($> 35^\circ$), where uncertainties due to projection effects would be high. This trend is not seen in other years even in deeper layers. It can be seen from the figure that the transition from southward to northward flow occur around a latitude of 5°N, rather than at the equator. It is not clear if this is real or due to some systematic effect. Komm et al. (2004) find the counter-cells in 2002 MDI data, though not in GONG data for the same duration. González Hernández et al. (2006) find counter-cell using GONG data in both north and south hemisphere and these counter-cells appear periodically with a period of one year that correlates with maximum values of the solar B_0 angle. Zaatri et al. (2006) have done a detailed analysis of correlation between flow velocities and the B_0 angle to identify and correct for the effect and find that after correction the counter-cells are present at high latitudes in near surface regions in both hemispheres. If these cells are real they will have consequences for the angular momentum transport as well as solar dynamo theories. More studies are needed to confirm or reject the existence of these cells. In addition to the counter-cell, other temporal variations have also been seen when the meridional flow pattern is averaged over an entire solar rotation. These variations can be studied us-

© 2006 WILEY-VCH Verlag GmbH & Co. KGaA, Weinheim

ing the residuals obtained by subtracting temporal averages from the observed values at each latitude. These residues are found to be of order of 10 m s^{-1} and some results show a systematic shift in the pattern. There is considerable disagreement between different results on the temporal variation of meridional flows and it is difficult to identify any robust pattern of temporal variations.

Ring diagram analysis has also been used to study flows associated with active regions. The dense-pack regions from MDI have been used by Hindman et al. (2004) and Haber et al. (2004) to make synoptic maps of sub-surface flows in the Sun. They find that flows tend to converge near active regions. Komm et al. (2005) found that active regions tend to rotate faster than their quieter surroundings. At depths greater than 10 Mm, they find strong outflows from active regions.

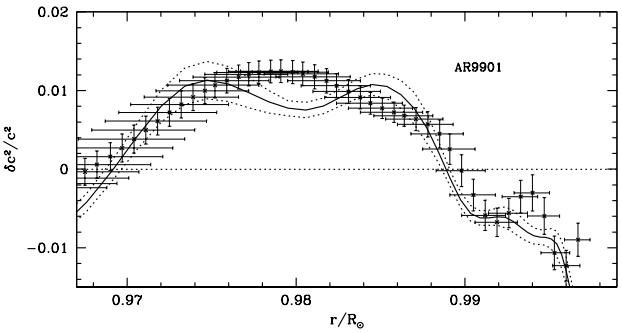

Fig. 5 The difference in sound speed between the region covering the active region NOAA9901 and a quiet region. The solid line shows the results obtained using the RLS inversion technique, with the dotted lines showing error estimates. The points with errorbars show the results using the SOLA inversion technique, with horizontal errorbars showing the resolution of the averaging kernels.

3.2 Solar structure

The frequencies of two different regions can differ if their internal structures are different. Frequency differences have been found between active and quiet regions on the Sun (Hindman et al. 2000; Rajaguru et al. 2001; Howe et al. 2004). The active regions are found to have higher frequencies, and the magnitude of the frequency differences appears to be correlated to differences in the average surface magnetic field between the corresponding regions. In addition to frequencies, the widths of the modes are also larger in active regions when compared to quiet regions, but the power in the modes is smaller (Rajaguru et al. 2001). There is also an increase in mode-asymmetry in active regions (Rajaguru et al. 2001). Similar variations have been seen in global mode characteristics as the average magnetic field increases with activity level (e.g., Libbrecht and Woodard 1990; Howe et al. 1999), though these variations are much smaller in magnitude as compared to those between active and quiet regions, presumably because of higher magnetic field.

The observed frequency differences between an active and a quiet region can be interpreted as structural difference that can be determined using inversion techniques described in Section 2.1. However, these neglect the direct effects of the magnetic fields, which cause frequency shifts due to additional force field. This is in addition to any structural changes induced by the magnetic field. It is not easy to distinguish between effect of magnetic field and that due to structural variations (Lin et al. 2006). Thus it is difficult to interpret these inversion results directly. Basu et al. (2004) found that in the immediate sub-surface layers, the sound speed is lower in active regions, but below a depth of about 7 Mm the trend reverses. This is similar to results found using time-distance technique (Kosovichev et al. 2000). Figure 5 shows the sound speed difference between the active region NOAA9901 and a quiet region as obtained using both the RLS and SOLA inversion techniques. Similar results are also found for the adiabatic index. The sound speed differences are of order of 1% in active regions with relatively strong magnetic field and these differences increase with increasing average magnetic field in the regions studied. Considering that ring diagram analysis involves an average over $15^\circ \times 15^\circ$ region around the sunspot, the actual structural variations in the sunspot could be much larger.

In addition to differences in structure between active and quiet regions, there are differences in structure between different latitudes. Asphericity in solar structure has been studied using frequency splittings in global modes (Antia et al. 2001) to find a region of enhanced sound speed at latitude of around 60° in outer part of the convection zone. Since the global modes have poor depth resolution near the surface, these results can be checked using ring diagram analysis, which provides information on high degree modes. Using frequency differences between regions at high latitudes and the equator, Basu et al. (2007) found that both sound speed and adiabatic index vary with latitude. Furthermore, they found larger latitudinal differences during high activity phases of the solar cycle. They also found some temporal variation of sound speed near the surface.

4 Summary

Over the last decade considerable advances have been made in ring diagram analysis of zonal and meridional flows. However, more work is needed to understand systematic errors which would hopefully resolve the differences between different results for e.g., temporal variations or north-south asymmetry in zonal flows, or the presence of counter-cells in meridional flows. Further work is also needed before we can exploit the full potential of ring-diagram analysis to study solar structure variations.

Acknowledgements. SB is partially supported by NASA grant NNG-06GD13G, and NSF grant ATM 0348837.

References

Anderson, E.R., Duvall, T.L., Jr., Jefferies, S.M.: 1990, ApJ 364, 699

© 2006 WILEY-VCH Verlag GmbH & Co. KGaA, Weinheim

Antia, H.M., Basu, S.: 1994, A&AS 107, 421
Antia, H.M., Basu, S., Hill, F., Howe, R., Komm, R.W., Schou, J.: 2001, MNRAS 327, 1029
Backus G.E., Gilbert J.F.: 1968, Geophys. J. Roy. Astr. Soc. 16, 169
Basu, S., Antia, H.M.: 1999, ApJ 525, 517
Basu, S., Antia, H.M.: 2000a, ApJ 541, 442
Basu, S., Antia, H.M.: 2000b, Solar Phys. 192, 469
Basu, S., Antia, H.M.: 2003, ApJ 585, 553
Basu, S., Antia, H.M., Tripathy, S.C.: 1999, ApJ 512, 458
Basu, S., Antia, H.M., Bogart, R.S.: 2004, ApJ 610, 1157
Basu, S., Antia, H.M., Bogart, R.S.: 2007, ApJ (in press), astro-ph/0609505
Bogart, R.S., Basu, S.: 2004, in Proc. SOHO14/GONG 2004 Workshop, ed. D. Danesy, ESA SP-559, 329
Dikpati, M., Charbonneau, P.: 1999, ApJ 518, 508
Durney, B.R.: 1993, ApJ 407, 367
Duvall, T.L., Jr., Jefferies, S.M., Harvey, J.W., Pomerantz, M.A.: 1993, Nature 362, 430
Dziembowski, W.A., Pamyatnykh, A.A., Sienkiewicz, R.: 1990, MNRAS 244, 542
Giles, P.M, Duvall, T.L., Jr., Scherrer, P.H., Bogart, R.S.: 1997, Nature 390, 52
Gizon, L., Birch, A. C.: 2005, LRSP 2, 6
González Hernández, I., Patrón, J.: 2000, Solar Phys. 191, 37
González Hernández, et al.: 1999, ApJ 510, L153
González Hernández, Komm, R., Hill, F., Howe, R., Corbard, T., Haber, D.A.: 2006, ApJ 638, 576
Gough, D.O., Thompson, M.J.: 1991, in Solar Interior and Atmosphere, (eds Cox, A. N., Livingston, W. C., Matthews, M., (Unix. of Arizona Press, Tucson) p. 519
Gough, D.O., et al.: 1996, Science 272, 1296
Haber, D.A., Hindman, B.W., Toomre, J., Bogart, R.S., Thompson, M.J., Hill, F.: 2000, Solar Phys. 192, 335
Haber, D.A., Hindman, B.W., Toomre, J., Bogart, R.S., Larsen, R. M., Hill, F.: 2002, ApJ 570, 855
Haber, D.A., Hindman, B.W., Toomre, J., Thompson, M.J.: 2004, Solar Physics, 220, 371
Hathaway, D.H., et al.: 1996, Science 272, 1306
Hill, F.: 1988, ApJ 333, 996
Hill, F.: 1989, ApJ 343, L69
Hill, F.: 1990, Solar Phys. 128, 321
Hindman, B., Haber, D., Toomre, J., Bogart, R.: 2000, Solar Phys. 192, 363
Hindman, B. W., Gizon, L., Duvall, T,L., Haber, D.A., Toomre, J.: 2004, ApJ, 613, 1253
Howard, R., LaBonte, B.J.: 1980, ApJ 239, L33
Howe, R., Komm, R., Hill, F.: 1999, ApJ 524, 1084
Howe, R., Christensen-Dalsgaard, J., Hill, F., Komm, R.W., Larsen, R.M., Schou J., Thompson M.J., Toomre J.: 2000, ApJ 533, L163
Howe, R., Komm, R.W., Hill, F., Haber, D.A., Hindman, B.W.: 2004, ApJ 608, 562
Komm, R., Corbard, T., Durney, B.R., González Hernández, I., Hill, F., Howe, R., Toner, C.: 2004, ApJ 605, 554
Komm, R., Howe, R., Hill, F., González Hernández, I., Toner, C., Corbard, T.: 2005, ApJ, 631, 636
Kosovichev, A.G., Duvall, T.L., Jr., Scherrer, P.H.: 2000, Solar Phys. 192, 159
Libbrecht, K.G., Woodard, M.F.: 1990, Nature 345, 779
Lin, C.-H., Li, L.-H., Basu, S.:2006, in Proc. SOHO18/GONG 2006/ HELAS I, Ed. K. Fletcher, ESA SP-624, in press
Nandy, D., Choudhuri, A.R.: 2002, Science 296, 1671
Nigam, R., Kosovichev, A.G.: 1998, ApJ 505, L51
Patrón, J., *et al.*: 1997, ApJ 485, 869
Pijpers, F.P., Thompson, M.J.: 1992, A&A 262, L33
Pijpers, F.P., Thompson, M.J.: 1994, A&A 281, 231
Rajaguru, S.P., Basu, S., Antia, H.M.: 2001, ApJ 563, 410
Schou, J., Bogart, R.S.: 1998, ApJ 504, L131
Schou, J., et al.: 1998, ApJ 505, 390
Thompson, M.J., et al.: 1996, Science 272, 1300
Zaatri, A., Komm, R., González Hernández, I., Howe, R., Corbard, T.: 2006, Solar Phys. 236, 227

© 2006 WILEY-VCH Verlag GmbH & Co. KGaA, Weinheim